Supplementary Information

Re-balancing Replica Exchange with Solute Tempering for Sampling Dynamic Protein Conformations

Yumeng Zhang, Xiaorong Liu*,# and Jianhan Chen*

Department of Chemistry
University of Massachusetts
Amherst, MA 01003, USA

* Corresponding Authors: Email: xrliu@umich.edu (XL), jianhanc@umass.edu (JC),
Phone: (413) 545-3386 (JC),
Current Address: Department of Chemistry, University of Michigan, Ann Arbor, MI 48109

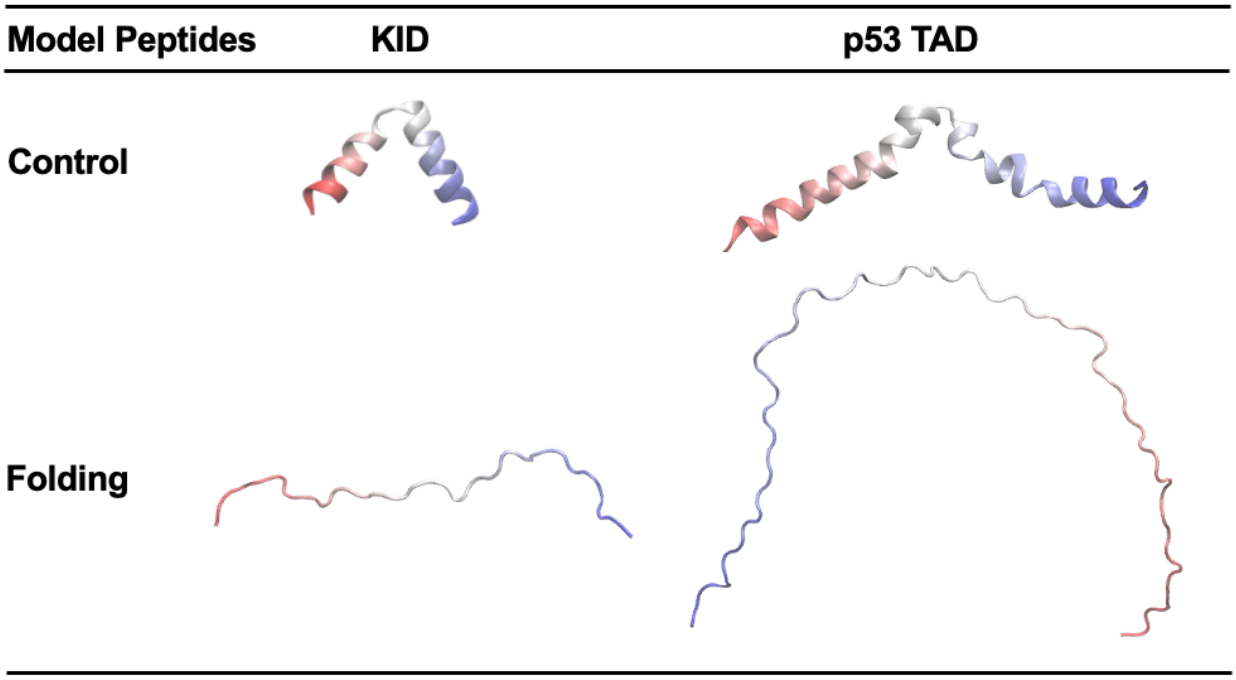

Figure S1. The initial conformations of KID and p53-NTD for folding and control simulations. The N-terminal region of the peptide is colored red and blue for the C-terminal region (following the red-white-blue, RWB color scheme).

Table S1. Summary of REST2 and REST3 simulations.

Protocols	**REST2 (298K-500K, 16-rep)**		**REST3 (298K-500K, 16-rep)**		**REST3 (298K-450K, 8-rep)**
	Control	**Folding**	**Control**	**Folding**	**Folding**
KID	1 *μs*	1 *μs*	1 *μs*	1 *μs*	
p53-NTD	2 *μs*	2 *μs*		2 *μs*	2 *μs*

Table S2. Parameters for REST2 and REST3 protocols used in this work. Note that for REST3, $\lambda_m^{pw,vdw} = \kappa_m \lambda_m^{pw}$

Rep	Temp (K)	REST2		κ_m	Rep	Temp (K)	REST2		κ_m
		λ_m^{pp}	λ_m^{pw}				λ_m^{pp}	λ_m^{pw}	
0	298	1	1	-	8	392	0.759	0.871	-
1	308	0.966	0.983	-	9	406	0.733	0.856	-
2	319	0.933	0.966	-	10	420	0.708	0.841	-
3	330	0.902	0.950	-	11	435	0.684	0.827	-
4	342	0.871	0.933	-	12	450	0.661	0.813	-
5	354	0.841	0.917	-	13	466	0.639	0.799	-
6	366	0.813	0.902	-	14	483	0.617	0.785	-
7	379	0.785	0.886	-	15	500	0.596	0.772	-
Rep	Temp (K)	REST3		κ_m	Rep	Temp (K)	REST3		κ_m
		λ_m^{pp}	$\lambda_m^{pw,vdW}$				λ_m^{pp}	$\lambda_m^{pw,vdW}$	
0	298	1	1	1.000	8	392	0.759	**0.823**	**1.025**
1	308	0.966	0.983	1.000	9	406	0.733	**0.882**	**1.030**
2	319	0.933	0.966	1.000	10	420	0.708	**0.871**	**1.035**
3	330	0.902	0.950	1.000	11	435	0.684	**0.860**	**1.040**
4	342	0.871	**0.938**	**1.005**	12	450	0.661	**0.850**	**1.045**
5	354	0.841	**0.926**	**1.010**	13	466	0.639	**0.839**	**1.050**
6	366	0.813	**0.915**	**1.015**	14	483	0.617	**0.829**	**1.055**
7	379	0.785	**0.904**	**1.020**	15	500	0.596	**0.818**	**1.060**
Rep	Temp (K)	REST3		κ_m	Rep	Temp (K)	REST3		κ_m
		λ_m^{pp}	$\lambda_m^{pw,vdW}$				λ_m^{pp}	$\lambda_m^{pw,vdW}$	
0	298	1	1	1.000	4	377	0.790	**0.907**	**1.020**
1	316	0.943	0.971	1.000	5	400	0.745	**0.886**	**1.027**
2	335	0.889	**0.946**	**1.003**	6	424	0.702	**0.867**	**1.035**
3	355	0.838	**0.924**	**1.010**	7	450	0.662	**0.850**	**1.045**

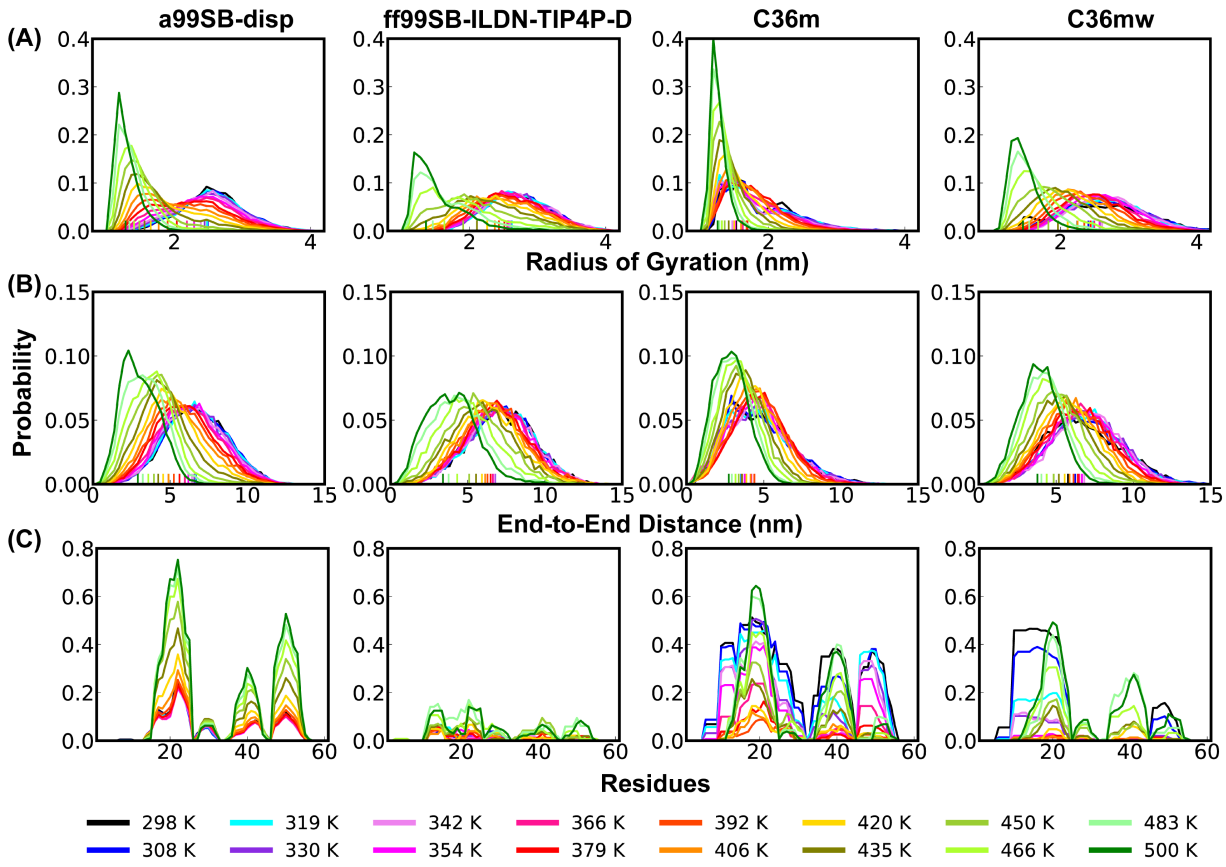

Figure S2. Distributions of radius of gyration (A) and end-to-end distance (B) and residue helicity profiles (C) of p53-NTD under all 16 conditions derived from REST2 folding and control simulations in four selected protein force fields. The colors for different effective temperature conditions are shown at bottom.

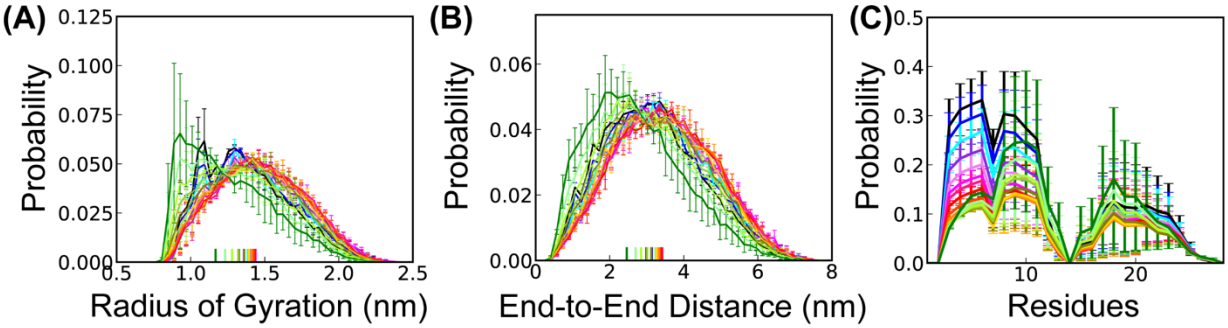

Figure S3. Distributions of radius of gyration (A) and end-to-end distance (B) and residue helicity profiles (C) of KID under all 16 conditions derived from REST2 control and folding simulations in a99sb-disp. Coloring of different effective temperature conditions is the same as Figure S2.

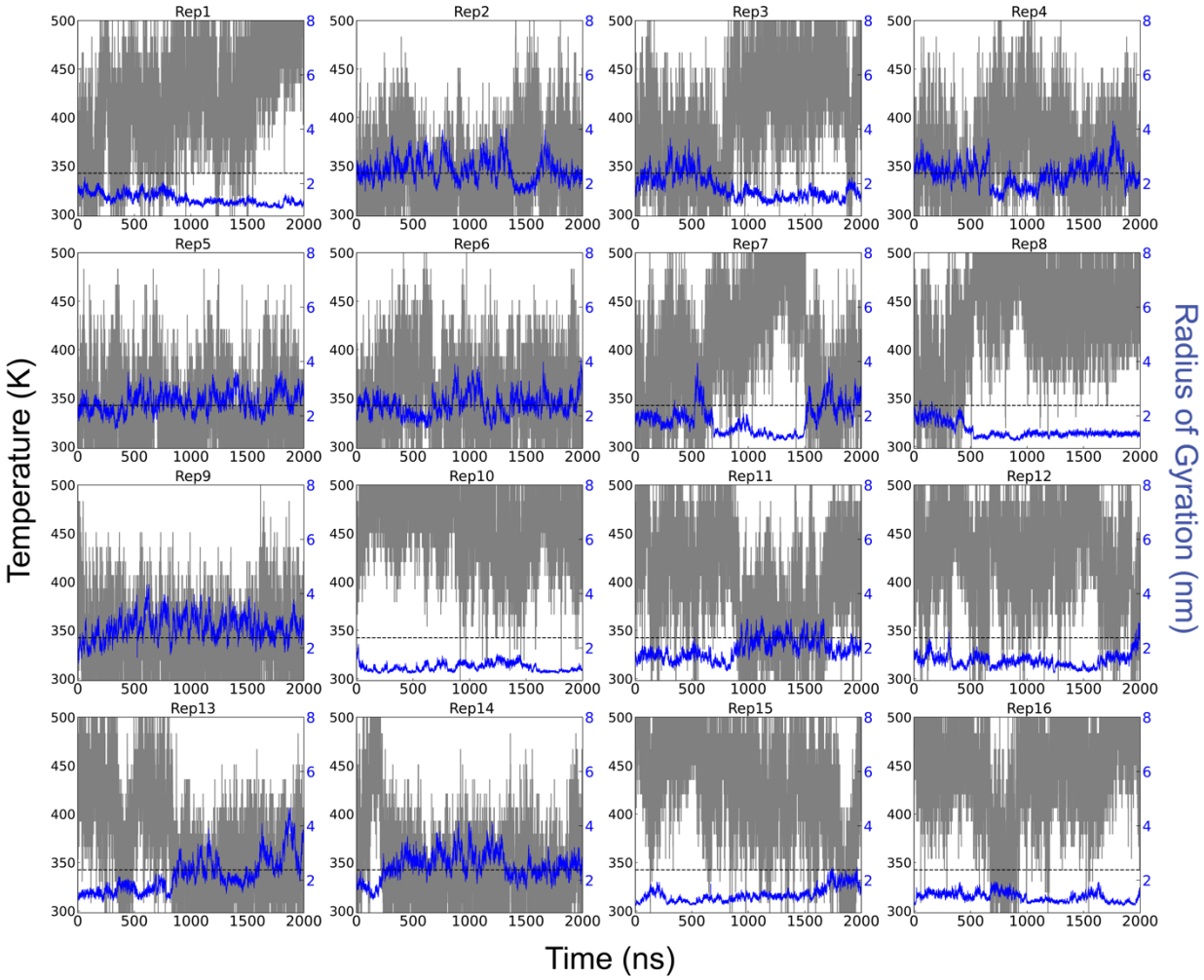

Figure S4. Evolution of temperature (grey) and radius of gyration (blue) for each of the 16 replicas of the REST2 control simulation of p53-NTD in a99SB-disp. The grey dashed line marks the radius of gyration from SAXS (2.39 nm).

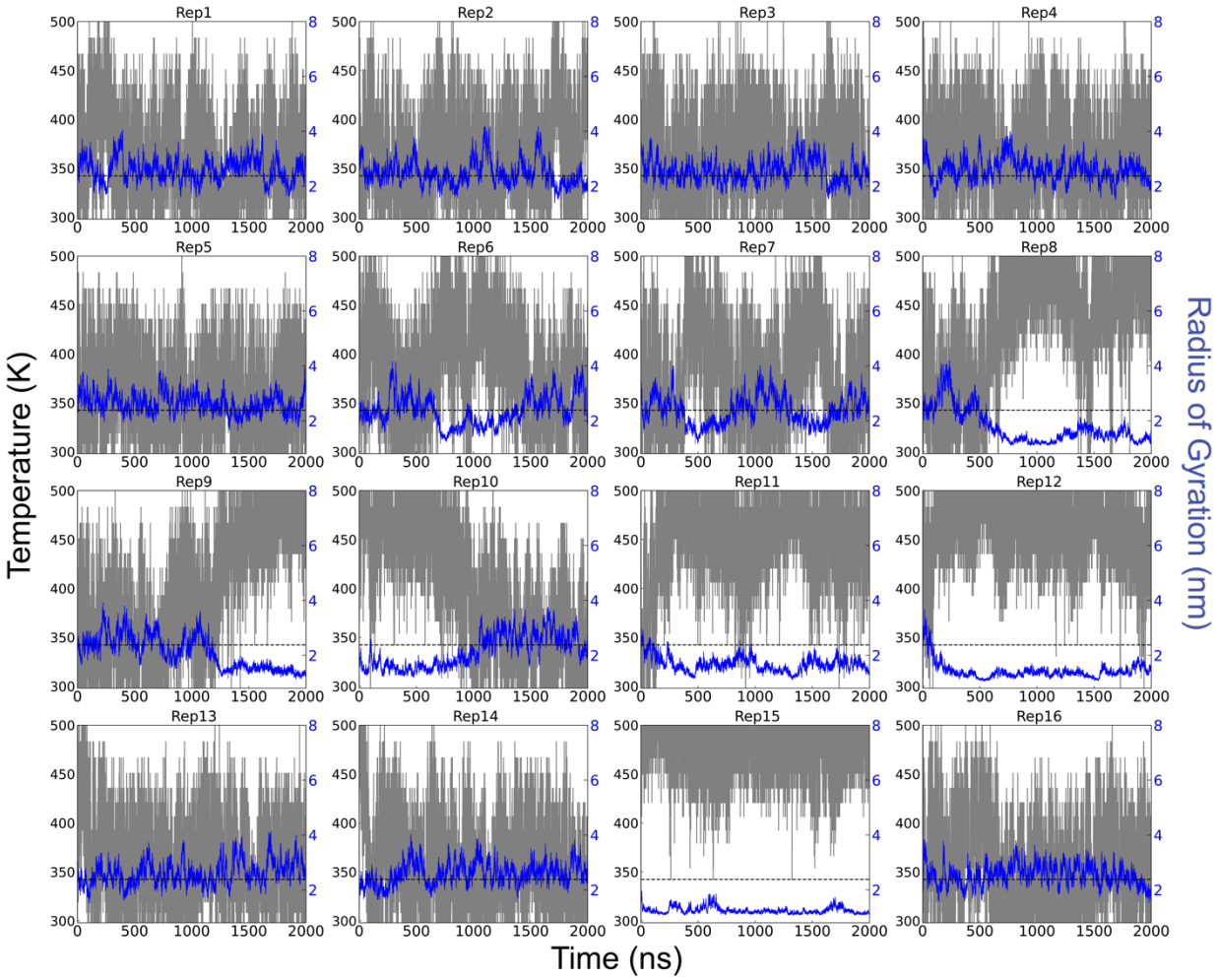

Figure S5. Evolution of temperature (grey) and radius of gyration (blue) for each of the 16 replicas of the REST2 folding simulation of p53-NTD in a99SB-disp. The grey dashed line marks the radius of gyration from SAXS (2.39 nm).

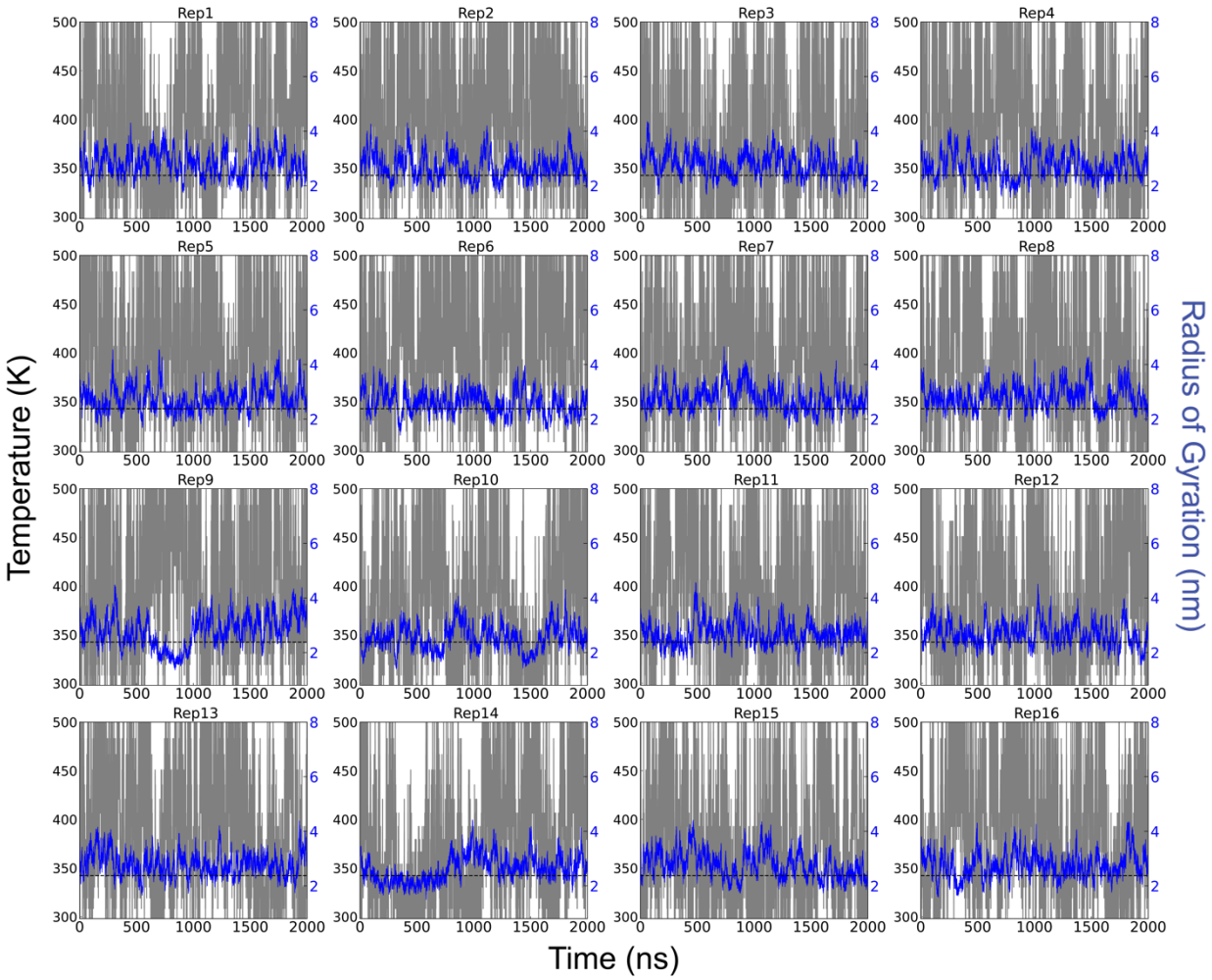

Figure S6 Evolution of temperature (grey) and radius of gyration (blue) for each of the 16 replicas of the REST3 folding simulation of p53-NTD in a99SB-disp. The grey dashed line marks the radius of gyration from SAXS (2.39 nm).

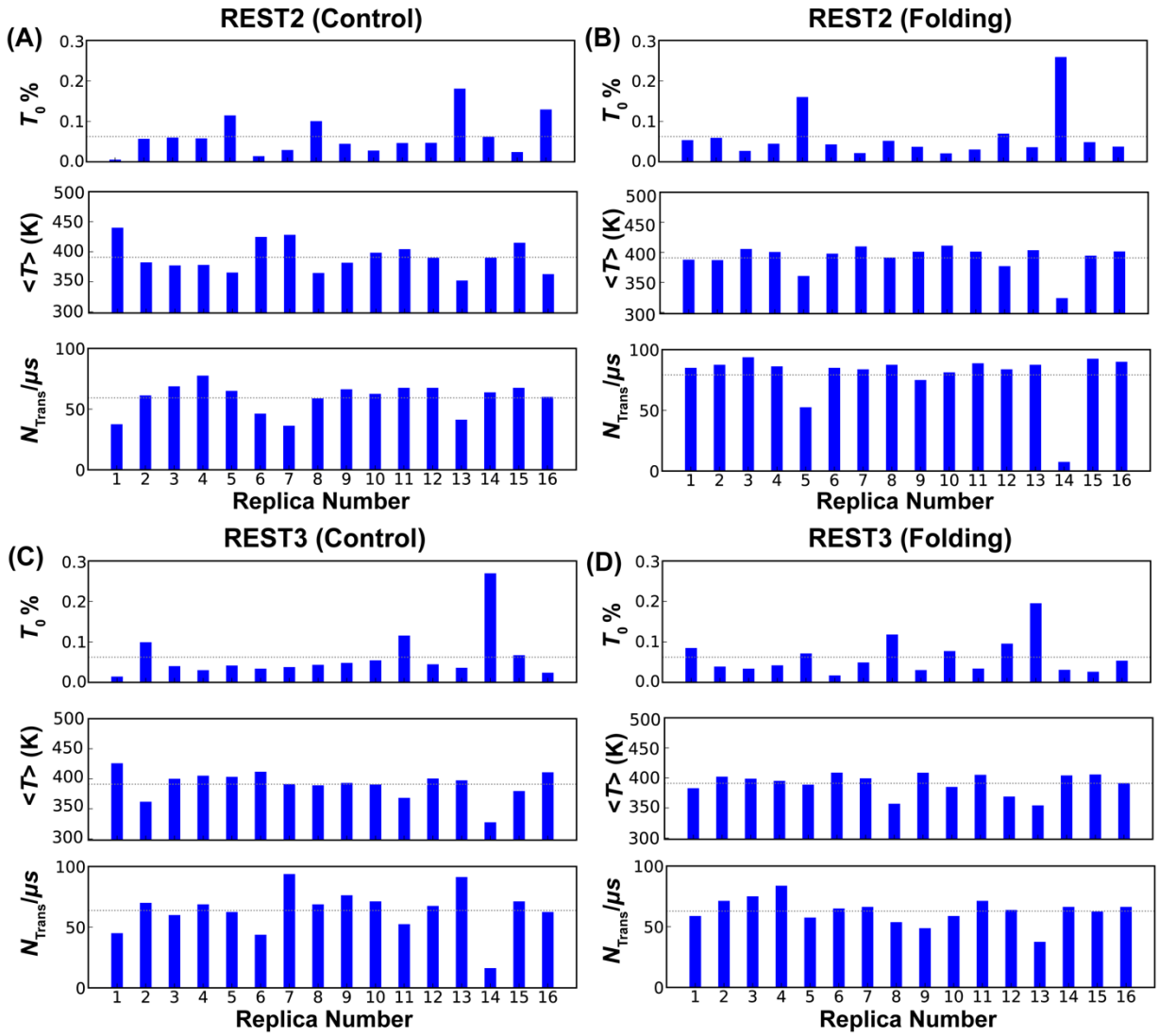

Figure S7. Efficiency of replica exchange of KID simulations with REST2 and REST3 control and folding simulations (Table S1), as reflected in occupancy at the lowest temperature (top, T_0, 298 K), average effective temperature, and the number of temperature round trip per *μs* for each replica. The average $N_{trans}/\mu s$ of all 16 replicas are 59.2/*μs* (A), 79.2/*μs* (B), 63.8/*μs* (C), and 62.9/*μs* (D) in REST2 and REST3 control and folding runs, respectively.

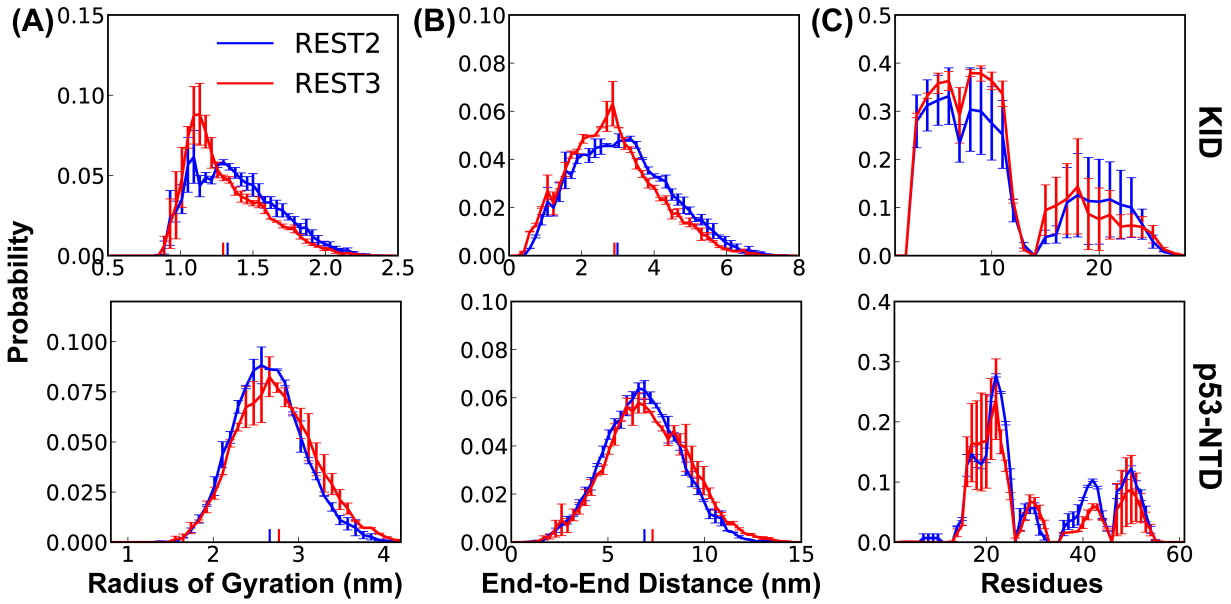

Figure S8. Distributions of radius of gyration (A), end-to-end distance (B), and average residue helicity profile (C) of KID (top) and p53-NTD (bottom) from REST2 (blue) and REST3 (red) simulations in a99SB-disp. The error bars were calculated from the differences between the folding and control runs for KID. The folding trajectories for p53-NTD (excluding the first 200 ns) were divided into two parts for error bar calculations.

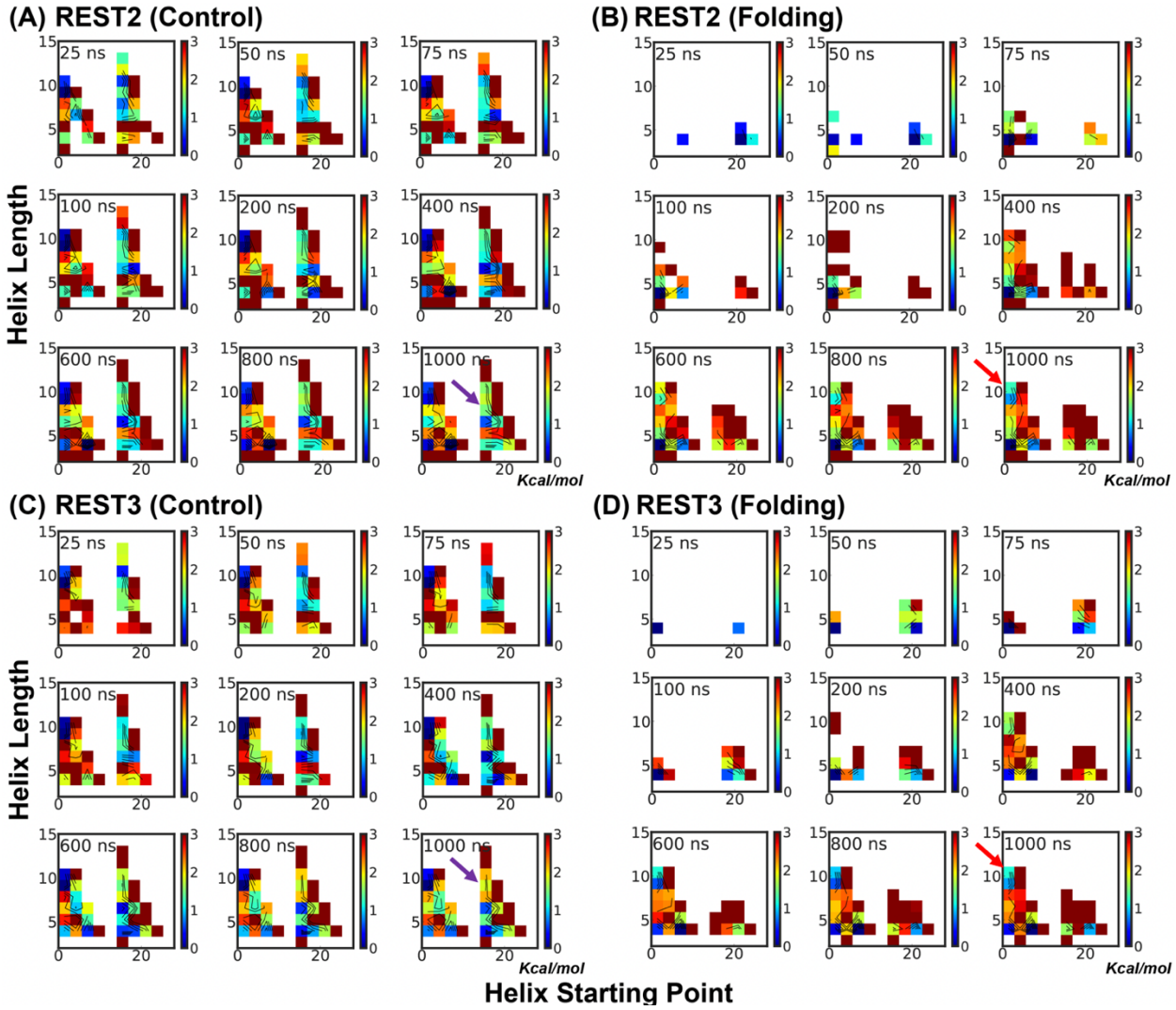

Figure S9. 2D probability distributions of the starting position and length of partial helices of KID at 298 K as a function of REST2 and REST3 simulation time. All probability distributions were first converted into free energy surface before plotting. Purple and red arrows highlight two helical substates with significant difference convergence rates in REST2 and REST3.

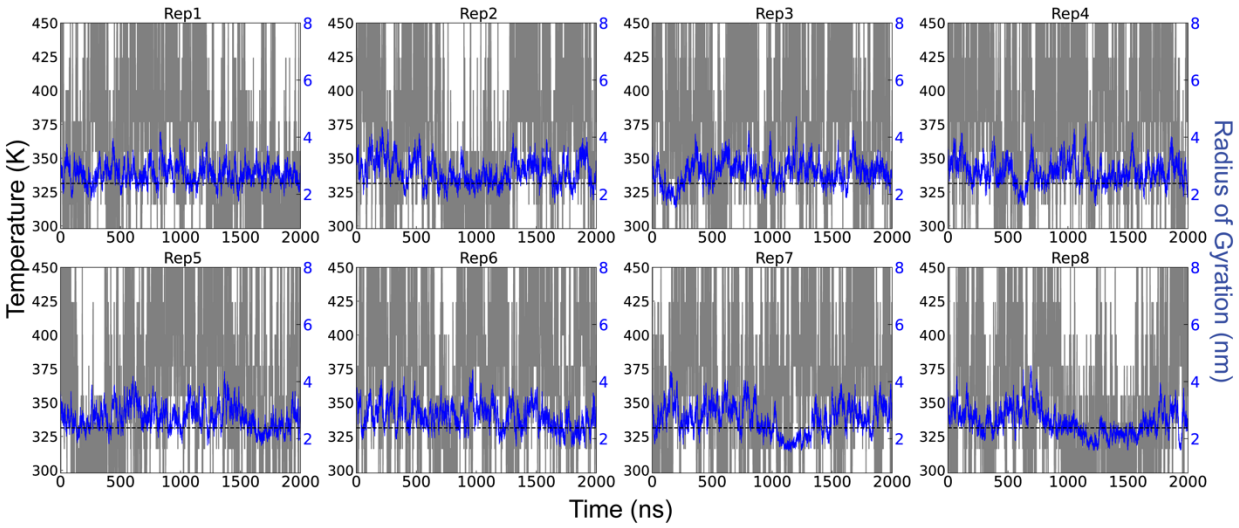

Figure S10. Evolution of temperature (grey) and radius of gyration (blue) for all replicas of the REST3 folding simulation of p53-NTD in a99SB-disp using 8 replicas. The grey dashed line marks the radius of gyration from SAXS (2.39 nm).

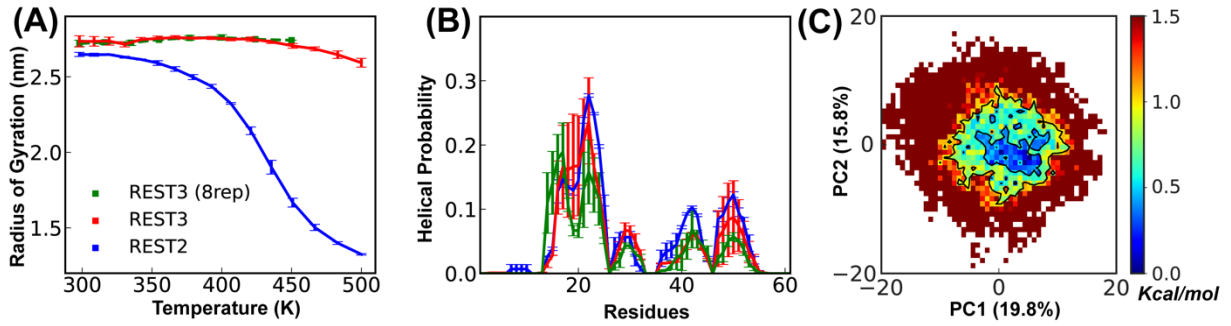

Figure S11. Properties of conformational ensembles as a function of effective temperature derived from RSET2 and REST3 simulations of p53-NTD (folding simulation) in a99SB-disp. These properties include average radius of gyration (A) and end-to-end distance (B). (C) Average residue helicity profiles at 298 K for p53-NTD calculated by three protocols. The 2 *μs* folding simulation excluding the first 200 ns trajectory was divided into two parts for error bar calculations.